Growth-rate dependent resource investment in bacterial motile behavior quantitatively follows potential benefit of chemotaxis

Bin Ni[a,b], Remy Colin[a,b], Hannes Link[a,b], Robert G. Endres[c,d], and Victor Sourjik[a,b,1]

[a]Max Planck Institute for Terrestrial Microbiology, 35043 Marburg, Germany; [b]LOEWE Center for Synthetic Microbiology (SYNMIKRO), 35043 Marburg, Germany; [c]Department of Life Sciences, Imperial College, SW7 2AZ London, United Kingdom; and [d]Centre for Integrative Systems Biology and Bioinformatics, Imperial College, SW7 2AZ London, United Kingdom

Edited by Simon A. Levin, Princeton University, Princeton, NJ, and approved November 26, 2019 (received for review June 24, 2019)

Microorganisms possess diverse mechanisms to regulate investment into individual cellular processes according to their environment. How these regulatory strategies reflect the inherent trade-off between the benefit and cost of resource investment remains largely unknown, particularly for many cellular functions that are not immediately related to growth. Here, we investigate regulation of motility and chemotaxis, one of the most complex and costly bacterial behaviors, as a function of bacterial growth rate. We show with experiment and theory that in poor nutritional conditions, *Escherichia coli* increases its investment in motility in proportion to the reproductive fitness advantage provided by the ability to follow nutrient gradients. Since this growth-rate dependent regulation of motility genes occurs even when nutrient gradients are absent, we hypothesize that it reflects an anticipatory preallocation of cellular resources. Notably, relative fitness benefit of chemotaxis could be observed not only in the presence of imposed gradients of secondary nutrients but also in initially homogeneous bacterial cultures, suggesting that bacteria can generate local gradients of carbon sources and excreted metabolites, and subsequently use chemotaxis to enhance the utilization of these compounds. This interplay between metabolite excretion and their chemotaxis-dependent reutilization is likely to play an important general role in microbial communities.

chemotaxis | selection | fitness cost | growth | metabolism

Bacterial responses to environmental changes range from adjustment of metabolism to induction of different stress protection mechanisms and tactic behavior. In most cases, there is an apparent qualitative benefit of investment into a cellular function under particular environmental conditions, e.g., uptake of a specific carbon source when it is available. However, demonstrating that a regulatory strategy exactly follows the physiological benefit of the respective cellular function remains challenging, although several recent studies suggested that allocation of metabolic resources may indeed optimize growth (1–6).

Most prokaryotes can swim by rotating flagellar filaments, powered by the proton motive force. Swimming bacteria can typically follow various chemical gradients in their environment, by modulating the frequency of cell reorientations (tumbles) dependent on their swimming direction relative to the gradient (7, 8). The core of the chemotaxis signaling pathway includes stimulus-specific chemoreceptors (Tar, Tsr, Trg, Tap, and Aer in *Escherichia coli*), which regulate the cytoplasmic histidine kinase CheA and thereby phosphorylation of the response regulator CheY. Phosphorylated CheY controls rotation of flagellar motor; in the case of *E. coli*, promoting its directional switching that induces tumbles. *E. coli* chemotaxis pathway further includes CheZ, the phosphatase of CheY, and the adaptation enzymes CheR and CheB.

Flagellar motility consumes several percent of total cellular protein and energy budget (9, 10), which is primarily spent for the biogenesis of flagella and powering of their rotation, respectively, and to a lesser extent for the chemotactic signaling. Consistent with this high cost of motility, expression of flagellar genes can significantly reduce growth (11). Nevertheless, *E. coli* motility is up-regulated in poor carbon sources, as a part of the regulon controlled by cyclic adenosine monophosphate (cAMP) and its receptor protein (CRP) (1, 12, 13). Although this investment strategy could potentially enhance chemotaxis-mediated nutrient uptake in heterogeneous environments (14), thus enabling risk-prone foraging behavior (12), under which conditions it might be advantageous remained unclear, particularly considering that selection pressure on motility and chemotaxis is environment specific (15).

In this study, we investigated the relation between costs and benefits of motility in *E. coli* cells grown in a number of carbon sources of different quality (Fig. 1*A*). Our results suggest that bacteria invest in swimming behavior in proportion to the fitness benefit provided by chemotaxis, both of which depend on the growth rate. This demand-dependent investment could be recapitulated by mathematical modeling that considers growth-dependent proteome partitioning, chemotaxis, and competition for nutrients. Tactic enhancement of nutrient utilization was observed in externally introduced or in self-generated gradients of nutrients, suggesting that it is important across a wide range of environments.

Significance

To which extent gene regulatory programs are optimized by evolution is one of the fundamental biological questions. Swimming motility is one of the costliest bacterial behaviors, but expression of motility genes nevertheless increases when bacteria grow slower on poor carbon sources. Here, we show that competitive fitness benefit provided by the ability of motile bacteria to follow gradients of secondary nutrients shows similar negative dependence on the growth rate as the investment in motility. Thus, bacteria appear to pre-invest into the motile behavior in proportion to the anticipated benefit that can be provided by chemotaxis when nutrient gradients become available in their environment.

Author contributions: B.N., R.C., H.L., R.G.E., and V.S. designed research; B.N., R.C., H.L., and R.G.E. performed research; B.N. and R.C. analyzed data; and B.N., R.C., H.L., R.G.E., and V.S. wrote the paper.

The authors declare no competing interest.

This article is a PNAS Direct Submission.

[1]To whom correspondence may be addressed. Email: victor.sourjik@synmikro.mpi-marburg.mpg.de.

This article contains supporting information online at https://www.pnas.org/lookup/suppl/doi:10.1073/pnas.1910849117/-/DCSupplemental.

First published December 23, 2019.

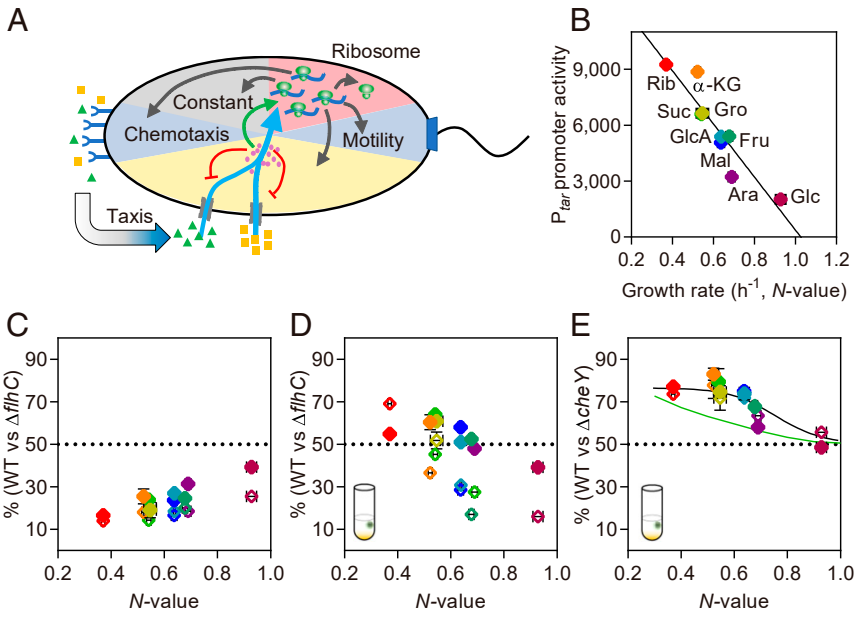

Fig. 1. Nutrient-dependent costs and benefits of motility in the presence of introduced gradients. (*A*) Schematics illustrating growth-rate dependent partitioning of the cellular protein budget into different functional sectors, as well as coutilization of 2 different nutrients (triangles and squares) regulated by cAMP (small circles). Also indicated is chemotaxis-mediated enhancement of nutrient uptake. (*B*) Relation between growth rate, denoted as nutritional (*N*-) value of the carbon source and motility gene expression. Cells were cultured with shaking (180 r.p.m.) in minimal medium containing different carbon sources as indicated (Rib: 20 mM ribose, α-KG: 12 mM α-ketoglutarate, Suc: 15 mM succinate, Gro: 0.4% glycerol, GlcA: 20 mM gluconate, Fru: 20 mM fructose, Mal: 0.2% maltose, Ara: 20 mM arabinose, Glc: 0.4% glucose). Expression of P_{tar}-GFP reporter and growth rate were measured at log phase of growth using plate reader (see *Methods* and *SI Appendix, Supplementary Text*). Solid line shows resource allocation model with 2 fitting parameters as detailed in *SI Appendix, Supplementary Text*; zero promoter activity is predicted at the *N*-value of 1.03. (*C* and *D*) Growth competition in the coculture of motile WT cells (expressing CFP) and nonmotile Δ*flhC* cells (expressing YFP), with *flhDC* expressed either under native promoter (solid diamonds) or under P_{tac} (open diamonds) promoter induced with 10 μM IPTG. Shown is fraction (in %) of the WT cells in a mixed population grown for 72 h without shaking in the absence (*C*) or in the presence (*D*) of a bead containing 12% casein hydrolysate. *N*-values were taken from *B*. (*E*) Same as *D*, but for competition between WT and Δ*cheY* cells. Solid lines show fit to the data using simulations of 2-compartment chemotaxis model (black) and prediction of the full 2D model (green) as detailed in *SI Appendix, Supplementary Text*. Cartoon in *D* and *E* illustrates emergence of gradients of casein hydrolysate from an introduced bead. In all competition experiments, both strains were initially inoculated at a 1:1 ratio.

Results

Growth-Rate Dependent Investment in Motility. We first assessed regulation of motility dependent on the growth rate, by culturing *E. coli* MG1655 Δ*flu* (deleted for the major surface adhesin to minimize cell aggregation) with shaking in different carbon sources. We observed that, similar to other cAMP-CRP regulated genes (5), activity of the chemotaxis (P_{tar}) or the flagellin (P_{fliC}) gene promoters showed a negative relationship with the growth rate (Fig. 1*B* and *SI Appendix*, Fig. S1*A*). The growth rate on a particular sole carbon source under these conditions of well-mixed culture was defined as the nutritional value of this carbon source (*N*-value), and it was used as a carbon source identifier throughout the manuscript. The up-regulation of motility genes at low *N*-value was reflected at the phenotypic level as a proportional increase of the cell swimming speed (*SI Appendix*, Fig. S1*B*) and of the chemotactic efficiency of a bacterial population (*SI Appendix*, Fig. S1*C*), which could be explained by the increased number (*SI Appendix*, Fig. S1*D*) and length (*SI Appendix*, Fig. S1*E*) of flagella.

We next used the mathematical model that is based on the previous theory of the growth-dependent protein resource allocation (5, 16) to describe how motility gene expression varies with the growth rate. This model assumes that a fixed finite size of the protein budget can either be dedicated to nutrient uptake or growth, i.e., protein synthesis, but trade-offs determine optimal growth rate (Fig. 1*A*, see *SI Appendix, Supplementary Text* for details). Indeed, the model could well reproduce the observed growth-rate dependence of motility gene expression (Fig. 1*B*, solid line).

Relative Fitness Cost of Motility Depends on Carbon Source. In order to directly evaluate the costs and benefits of motility as a function of the *N*-value, we used pairwise growth competition between strains to assess their relative reproductive fitness under particular conditions (11, 17). To monitor the ratio of 2 strains in cocultures using flow cytometry, we respectively labeled them with either cyan or yellow fluorescent proteins, CFP or YFP (*SI Appendix*, Fig. S2 *A* and *B*). This differential labeling had no direct effect on the relative fitness of bacteria (*SI Appendix*, Fig. S2*C*). Unless specified otherwise, the relative numbers of the 2 competing strains were determined in the early stationary phase (at 72 h) and thus reflect cumulative differences in growth over the entire duration of coculturing.

When the wild type (WT) was cocultured with Δ*flhC*, a knockout of the master transcription activator required for expression of all motility genes, Δ*flhC* consistently outgrew the WT cells, both without (Fig. 1*C* and *SI Appendix*, Fig. S2 *A* and *B*) and with (*SI Appendix*, Fig. S2*D*) stirring of the culture. Moreover, the fraction of WT cells decreased steadily as the *N*-value became lower (Fig. 1*C* and *SI Appendix*, Fig. S2*D*), which means that the relative fitness cost of motility, i.e., growth disadvantage of WT relative to Δ*flhC* cells in the coculture, becomes increasingly high at lower nutrient quality. A nearly identical result was obtained for the competition of the WT with Δ*fliC* mutant that lacks only flagellin (*SI Appendix*, Fig. S2*E*), demonstrating that the fitness cost of motility is primarily due to the biosynthesis of flagella (11). Nevertheless, flagellar rotation is also apparently costly since the WT was outcompeted by flagellated but nonmotile Δ*motAB* cells (*SI Appendix*, Fig. S2*F*).

To test whether the increased relative fitness cost of motility at low *N*-values is due to the elevated expression of flagellar genes, we placed the *flhDC* operon encoding transcriptional activator of the entire flagellar regulon under control of the synthetic P_{tac} promoter that is inducible by β-D-thio-galactoside (IPTG), but independent of cAMP-CRP regulation (18). Although in this background the expression of motility genes could be elevated above their native levels and largely decoupled from the growth rate (*SI Appendix*, Fig. S2*G*), the fitness cost of motility remained proportional to gene expression (*SI Appendix*, Fig. S2*H*).

Competitive Advantage of Chemotaxis in Presence of Introduced Nutrient Gradients. To explore the potential fitness benefits of motility and chemotaxis under conditions of competitive growth, nutrient gradients were introduced into the unstirred culture by using small (40 μL) agarose beads that contain 12% casein hydrolysate, a mixture of amino acids (*SI Appendix*, Fig. S3*A*). In the presence of these gradients and in poor carbon sources, the fraction of WT cells in the coculture with Δ*flhC* strain was >50% (Fig. 1*D* and *SI Appendix*, Fig. S3*B*), suggesting that the ability to locate nutrient gradients exceeded the high fitness cost of motility. In contrast, in carbon sources with high *N*-value, motility remained overall disadvantageous, despite its comparatively low fitness cost.

Confirming that this advantage of motility in the presence of nutrient gradients was due to chemotaxis, the WT outcompeted the motile but nonchemotactic Δ*cheY* strain in the same growth-rate dependent manner (Fig. 1*E*). Since these 2 strains have similar investment in motility, the competitive reproductive fitness advantage of the WT relative to Δ*cheY* provides a direct measure for the relative fitness benefit provided by chemotaxis under our experimental conditions. Swimming itself provided no advantage but rather carried significant cost, as Δ*cheY* strain was outcompeted by the flagellated but nonmotile Δ*motAB* strain (*SI Appendix*, Fig. S3*C*). Importantly, a similar growth-rate dependent advantage of motility and chemotaxis was observed in P_{tac}*_flhDC* background (Fig. 1 *D* and *E*), despite a very different dependence of gene expression on the carbon source (*SI Appendix*, Figs. S2*G* and S3*D*). This demonstrates that the increased benefit of chemotaxis in poor carbon sources is due to the increased importance of following nutrient gradients rather than to the higher investment in motility.

We next investigated how relative fitness benefit provided by chemotaxis depends on the concentration of the secondary nutrient. For *E. coli* grown on ribose, it exceeded the fitness cost of motility for the levels of casein hydrolysate in beads above 5% (*SI Appendix*, Fig. S3*B*). This corresponds to ∼20 mM aspartate and 10 mM serine, the 2 strongest attractants and at the same time preferentially consumed amino acids for *E. coli* (19). This fitness benefit of chemotaxis was nearly identical in experiments with 5% and 12% casein hydrolysate in beads over the entire range of the *N*-values (*SI Appendix*, Fig. S3*E*). In poor carbon sources, the trade-off between this benefit and the cost of motility was also similar for both these levels of casein hydrolysate (*SI Appendix*, Fig. S3*G*). However, at higher *N*-values where chemotaxis generally confers less benefit, the cost of motility apparently exceeds the benefit of chemotaxis toward lower levels of casein hydrolysate (*SI Appendix*, Fig. S3*G*). Consistently, this balance between the relative fitness cost of motility and benefit of chemotaxis was affected by up-regulation of flagellar genes, using P_{tac}*_flhDC* construct: Although the benefit of chemotaxis remained the same or even increased slightly in the P_{tac}*_flhDC* background (Fig. 1*E* and *SI Appendix*, Fig. S3*F*), it was apparently overweighed by the higher cost of motility for most carbon sources, particularly at the lower level of casein hydrolysate (Fig. 1*D* and *SI Appendix*, Fig. S3*H*).

Computational modeling was then used to rationalize how the advantage provided by chemotaxis to the secondary nutrient depends on the *N*-value of the primary carbon source (Fig. 1*A* and *SI Appendix*, Fig. S4 *A* and *B* and *Supplementary Text*). Growth was described using the previously proposed model (20), which predicts the growth rate on 2 coutilized nutrients based on the growth rates on individual substrates. The primary carbon source was initially spatially homogeneous, while the secondary nutrient formed a gradient (*SI Appendix*, Fig. S4*A*). The *N*-value of the secondary nutrient, 1.0 h^{-1}, was in the range of the growth rates observed at varying concentrations of casein hydrolysate (*SI Appendix*, Fig. S4*C*). Chemotactic cells were assumed to both spread due to random swimming and follow nutrient gradients, while nonchemotactic ones only spread randomly. Both cell types grew at the same rate on given nutrients. Here we simulated 2 different models: First, we described the process of gradient formation and chemotaxis using full spatial 2-dimensional (2D) simulations based on partial differential equations (PDEs; see *SI Appendix*, *Supplementary Text*), where the second nutrient leaked at constant rate from one side of the simulation box, mimicking diffusion out of the bead (*SI Appendix*, Fig. S4 *B* and *G*). Since the simulated gradient of secondary nutrient was confined to the immediate proximity of its source (*SI Appendix*, Fig. S4*G*), we also used a simplified model based on ordinary differential equations (ODEs) to fit experimental data. In this latter model, space is divided into 2 compartments, with the second nutrient being confined to one compartment while cells moved between the 2 compartments. Simulations of both models could qualitatively (prediction of the PDE model) and even quantitatively (data fitting by the ODE model) reproduce the observed dependence of the benefit of chemotaxis on the *N*-value (Fig. 1*E*). In our simulations, the reproductive fitness benefit of being able to localize the regions with higher concentration of the secondary nutrient is larger at low *N*-values, because in poor carbon sources the secondary nutrient is comparatively more nutritionally advantageous (*SI Appendix*, Fig. S4*D*). Consistent with experimental results (Fig. 1*E*), this dependence on the *N*-value was observed even without taking into consideration dependence of motility on the carbon source.

Competitive Advantage of Chemotaxis in Absence of Introduced Gradients. Surprisingly, we observed that chemotaxis could benefit bacteria even without imposed nutrient gradients, as revealed when coculturing the WT with Δ*cheY* or with similarly nonchemotactic Δ*cheB* strain without shaking (Fig. 2*A* and *SI Appendix*, Fig. S5*A*). The competitive advantage of the WT largely decreased at moderate mixing and was entirely abolished at strong mixing (Fig. 2*B*), indicating that it is caused by—apparently self-generated—gradients of nutrients. Equal reproductive fitness of the WT and Δ*cheY* cells in the stirred culture further confirms that the cost of the chemotactic signaling, incurred by the CheY phosphorylation cycle, is negligible compared to the overall cellular energy budget. In the unstirred culture, the enrichment of the WT was comparable in magnitude to the one observed in the presence of imposed gradients (Fig. 1*E* and *SI Appendix*, Fig. S3*E*), and it again decreased with the increasing *N*-value of the carbon source (Fig. 2*A*).

Nearly identical dependence of the relative fitness benefit of chemotaxis on the *N*-value was observed when motility genes were expressed under control of the P_{tac} promoter (Fig. 2*A*). Thus, as in the case of introduced gradients (Fig. 1*E*), the increased relative fitness benefit at low *N*-values is not the consequence of up-regulation of motility but rather due to the increased importance of chemotaxis in poor carbon sources. Despite this apparent lack of causality, we observed that the investment in motility in the WT cells showed strong positive correlation with the benefit of chemotaxis (Fig. 2*C*). Since this correlation was much less pronounced in the P_{tac}*_flhDC* background where flagellar expression was decoupled for the native regulation (*SI Appendix*, Fig, S5*B*), we hypothesized that bacteria naturally regulate investment

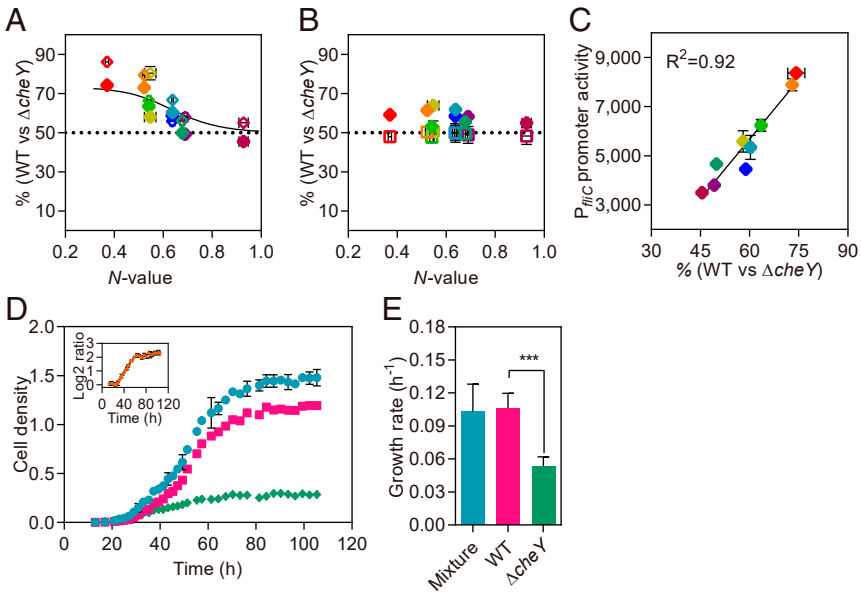

Fig. 2. Chemotaxis provides selective advantage even without introduced gradients. (*A*) Growth competition between WT and Δ*cheY* cells, performed as in Fig. 1. Cocultures were grown without shaking and in the absence of introduced gradients. *flhDC* was expressed either under native promoter (solid diamonds) or under P_{tac} (open symbols) promoter induced with 10 μM IPTG. *N*-values were taken from Fig. 1*B*. Solid line shows fit to the data using simulations of 2-compartment chemotaxis model (*SI Appendix, Supplementary Text*). (*B*) Same as *A* for *flhDC* expressed under native promoter, but under moderate (120 r.p.m., solid diamonds) or strong (180 r.p.m., open squares) mixing. (*C*) Correlation between motility gene expression in different carbon sources (from *SI Appendix*, Fig. S1*A*) and the relative fitness advantage of chemotactic cells (from *A*). Solid line is a linear fit to the data. (*D* and *E*) Growth of WT and Δ*cheY* cells in the coculture on ribose as sole carbon source without shaking (*D*), as well as corresponding growth rates (*E*). ***$P < 0.01$ in 2-tailed *t* test. In *D*, densities of WT (red squares) and Δ*cheY* cells (green diamonds) were calculated based on the measured density (OD_{600}) of the coculture (teal circles) and the ratio between WT and Δ*cheY* cells (*Inset*) determined using flow cytometry (see *Methods* and *SI Appendix, Supplementary Text*).

in motile behavior to be proportional to the potential benefit provided by chemotaxis (see *Discussion*).

To further understand whether the relative fitness benefit of chemotaxis in the absence of introduced gradients is limited to a specific growth stage, we used flow cytometry to measure the composition of the coculture during growth on ribose (Fig. 2*D*), α-ketoglutarate (*SI Appendix*, Fig. S6*A*), gluconate (*SI Appendix*, Fig. S6*B*), or glucose (*SI Appendix*, Fig. S6*C*). The WT cell fraction increased steadily throughout the early (*SI Appendix*, Fig. S6 *A*, *Inset*) or entire (Fig. 2 *D*, *Inset* and *SI Appendix*, Fig. S6 *B*, *Inset*) growth phase, with WT cells growing almost twice as fast as Δ*cheY* cells on ribose (Fig. 2*E*). No significant difference between the WT and Δ*cheY* was observed during growth on glucose (*SI Appendix*, Fig. S6*C*), confirming that at high *N*-value chemotaxis

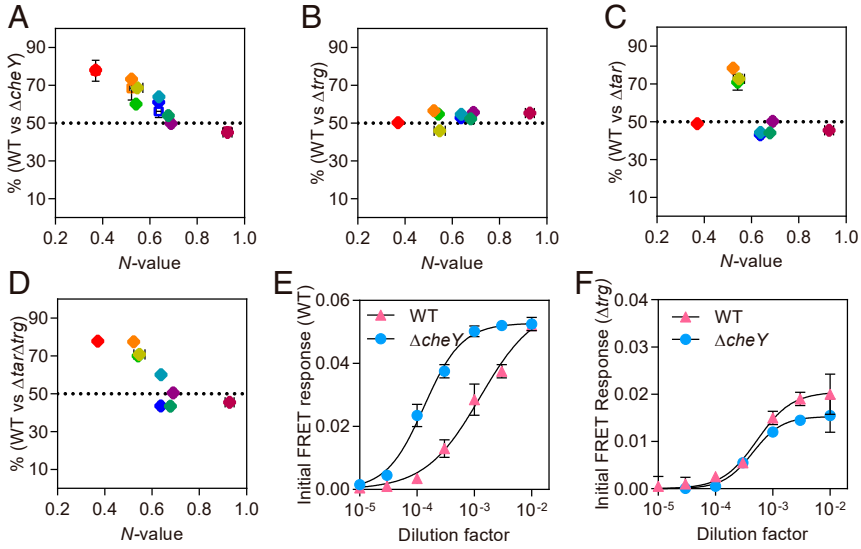

Fig. 3. Gradients of carbon sources and extracellular metabolites explain fitness advantage of chemotaxis. (*A*) Growth competition between WT and Δ*cheY* cells performed as in Fig. 2*A*, but in medium sealed with heavy mineral oil (solid diamonds) or under anaerobic conditions (open squares). (*B* and *C*) Growth competition between WT and Δ*trg* (*B*), Δ*tar* (*C*), or Δ*trg*Δ*tar* (*D*) cells, performed as in Fig. 2*A*. *N*-values were taken from Fig. 1*B*. (*E* and *F*) Chemotactic response of WT (*E*) or Δ*trg* (*F*) strains toward supernatant of WT or Δ*cheY* cultures measured by FRET (*SI Appendix, Supplementary Text* and Fig. S8 *A–D*).

provides no competitive advantage. Importantly, even during growth on ribose no advantage of chemotaxis could be seen when the 2 strains were incubated separately, and in that case Δ*cheY* cells even grew to slightly higher density in the stationary phase (*SI Appendix*, Fig. S6 *D* and *E*).

Gradients of Carbon Sources and Excreted Metabolites Could Explain Advantage of Chemotaxis. We hypothesized that chemotaxis enables WT bacteria to follow beneficial (most likely nutrient) gradients that transiently emerge in unstirred bacterial cultures. Oxygen could be excluded as a possible gradient source, since sealing the cocultures with heavy mineral oil to prevent aeration, or growing them under anaerobic conditions, had no significant effect on the relative fitness benefit of chemotaxis (Fig. 3*A*). Consistently, disruption of the aerotaxis receptor Aer yielded no competitive disadvantage in the coculture with the WT cells (*SI Appendix*, Fig. S7*A*). Furthermore, no advantage was observed for the WT cells competed against strains individually deleted for genes that encode chemotaxis receptors Tap (*SI Appendix*, Fig. S7*B*), Tsr (*SI Appendix*, Fig. S7*C*), or Trg (Fig. 3*B*), in any of the used carbon sources including ribose, the established ligand of Trg. In contrast, cells lacking Tar had clear competitive disadvantage relative to the WT in several carbon sources, which was comparable to the disadvantage of the general chemotaxis mutant Δ*cheY* (Figs. 2*A* and 3*C*).

Although the WT and Δ*tar* strains grew similarly when cocultured on ribose (Fig. 3 *B* and *C*), the WT had clear advantage during growth on these carbon sources when competed against the strain lacking both Tar and Trg (Fig. 3*D*). These results indicate emergence of 2 types of transient gradients within the culture: those of carbon sources and of excreted extracellular metabolites. The importance of both types of gradients could explain why during growth on ribose, either the ribose-specific receptor Trg or Tar that does not detect ribose but presumably responds to excreted metabolites, could individually mediate the advantage of chemotaxis.

We speculated that the ensuing higher efficiency of resource exploitation provides competitive advantage to the chemotactic bacteria in the coculture, enabling them to actively withdraw nutrient resources from the nonchemotactic cells, and that this fitness benefit provided by chemotaxis increases with the extent of nutrient limitation. In the absence of competition, however, nonchemotactic cells can eventually consume these nutrients and thus achieve similar growth. To test whether the lack of chemotaxis might indeed result in a less efficient consumption of the carbon source, we used a previously described assay of the pathway activity based on the Förster (fluorescence) resonance energy transfer (FRET) (21) to compare chemotactic response of the WT cells to supernatant derived from either WT or Δ*cheY* cultures. The WT cells, but not Δ*trg* cells, responded much more sensitively to the Δ*cheY* supernatant than to the WT supernatant (Fig. 3 *E* and *F* and *SI Appendix*, Fig. S8 *A–D*), indicating that the former indeed contains significantly higher levels of a Trg ligand—most likely less efficiently consumed ribose. Chemotaxis toward the carbon source gradients could also at least partly account for the Tar-dependent competitive advantage during growth on succinate, α-ketoglutarate, and glycerol (Fig. 3*C*), since Tar mediates attractant responses to all of these compounds (*SI Appendix*, Fig. S8 *E–G*). In contrast, Tsr apparently mediates repellent response to succinate and α-ketoglutarate (*SI Appendix*, Fig. S8 *H–J*), which might explain why during growth on these 2 carbon sources the deletion of *tsr* even increases the advantage of chemotaxis (*SI Appendix*, Fig. S7*C*).

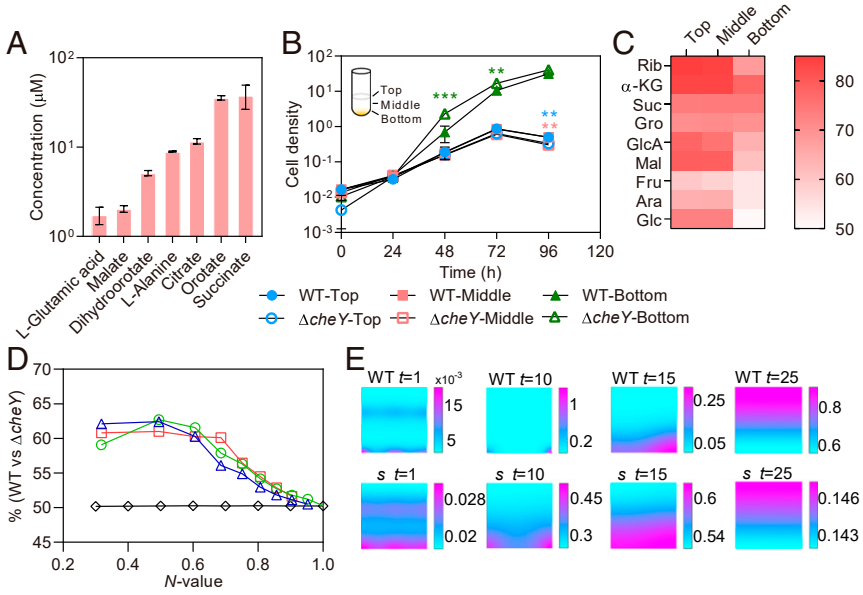

Fig. 4. Metabolic profile of the culture medium and emergence of gradients. (*A*) Extracellular metabolites secreted in the culture medium by WT cells grown without shaking with ribose as the sole carbon source for 60 h. Metabolites were analyzed by liquid chromatography–mass spectrometry (*SI Appendix, Supplementary Text*). (*B*) Time dependence of densities (OD_{600}) of WT (solid symbols) or Δ*cheY* (open symbols) cells grown individually without shaking, with ribose as the sole carbon source, in the top (circles), middle (squares), and bottom (triangles) layers of the liquid culture. $^{**}P < 0.05$, $^{***}P < 0.01$ in 2-tailed *t* test. (*C*) Proportion of WT cells in different layers of the cocultures with Δ*cheY* cells grown for 72 h without shaking with indicated carbon sources. (*D*) Full 2D simulations of competition between the WT and Δ*cheY* cells cocultured on different primary nutrients and excreting secondary nutrients as detailed in *SI Appendix, Supplementary Text*. Shown are simulations for chemotactic response to only primary nutrient (black open diamonds), to both primary and secondary nutrients (blue open triangles), and to only secondary nutrient (green open circles), with chemotactic sensitivity varying dependent on the carbon source as in *SI Appendix*, Fig. S1*C*. Also shown is the simulation with chemotactic response to both primary and secondary nutrients but with constant high sensitivity of chemotaxis, simulating motility induction under P_{tac} promoter (red open squares). (*E*) Spatial maps of WT cell density (*Top*, in units of OD) and of concentration of secondary nutrient *s* (*Bottom*, in millimolar), for indicated time points (*t* in hours) and for *N*-value of the primary nutrient 0.3 h^{-1}.

Succinate Is a Major Excreted Chemoattractant. Following gradients of extracellular metabolites excreted by bacteria themselves appears to be comparably important for the observed fitness benefit. Such chemotaxis toward extracellular metabolites—mediated by Tar—could explain why Δ*trg* cells compete equally with the WT during growth on ribose (Fig. 3*B*), despite clearly lacking response to this sugar (*SI Appendix*, Fig. S8 *K–M*). It is also likely to explain the advantage of chemotaxis during growth on carbon sources that do not themselves elicit a chemotactic response, such as gluconate (*SI Appendix*, Fig. S8 *M* and *N*).

Consistent with this hypothesis, we detected comparatively high (10–100 μM) levels of several potential chemoattractants and nutrients in the culture supernatant of WT cells growing on ribose, α-ketoglutarate, gluconate, or glucose (Fig. 4*A* and *SI Appendix*, Fig. S9*A* and Datasets S1 and S2), and culture supernatant could both elicit a chemotactic response (Fig. 3*E*) and enhance growth of an *E. coli* culture (*SI Appendix*, Fig. S9*B*) at dilutions of up to 10^{-3} to 10^{-4}. In particular, high levels of succinate, which is sensed by *E. coli* as a chemoattractant at concentrations above 1 μM (*SI Appendix*, Fig. S8*F*), were excreted by ribose-, gluconate- or glucose-fed cells (Fig. 4*A* and *SI Appendix*, Fig. S9*A*). Secretion of succinate indicates that, under our conditions, these carbon sources are at least partly catabolized via mixed acid fermentation (22), presumably due to low levels of oxygen in the unstirred culture. Addition of 5 mM succinate was observed to promote culture growth, dependent of the *N*-value of the primary carbon source (*SI Appendix*, Fig. S9*C*). It further seems that succinate and several other extracellular metabolites are secreted into the culture medium and not released from lysing cells, since levels of these compounds were similar in the supernatant and in the sample from the whole culture broth (*SI Appendix*, Fig. S9*D*). Levels of external succinate were lower in the α-ketoglutarate-fed cultures, but high levels of another potent Tar-specific chemoattractant, L-glutamate, were detected instead (*SI Appendix*, Fig. S9*A*).

Emergence of Nutrient and Cell Gradients in the Culture. How gradients of carbon sources and extracellular metabolites emerge in the culture? One possible origin of transient gradients, predicted by a previous theoretical study (14), could be local fluctuations in the nutrient consumption by bacteria. Another likely origin is gradual sedimentation of bacteria, which is common in aquatic habitats and could establish a nonuniform profile of cell density and therefore of nutrient consumption in the unstirred culture. Consistent with this second scenario, an increasing fraction of bacteria could be found in the sediment at the later stages of culture growth (Fig. 4*B*). This fraction was significantly smaller in the WT than in the Δ*cheY* culture, indicating that chemotaxis in emergent gradients reduces sedimentation of the WT cells. This difference was even more pronounced in the coculture, where the fraction of the WT was markedly higher in the upper layers of the culture than near the sediment (Fig. 4*C*).

To better understand this interplay between emergent gradients of secreted and consumed metabolites and chemotaxis, we modified our numerical models to include excretion of the secondary nutrient as a byproduct of the carbon source consumption (*SI Appendix*, Fig. S10 and *Supplementary Text*). This secondary nutrient is then coutilized along the primary nutrient for growth. In the full 2D simulations, cell sedimentation due to gravity was also explicitly considered. We observed that chemotaxis toward the secondary nutrient was alone sufficient to gain an *N*-value dependent competitive growth advantage (Fig. 4*D*). The 2-compartment ODE model that considered only chemotaxis toward the secondary nutrient and assumed constant chemotactic efficiency could then be used to quantitively reproduce experimental data (Fig. 2*A*). Notably, nearly identical advantage of chemotaxis was observed when the efficiency of motility and chemotaxis was assumed to depend on the *N*-value (Fig. 4*D*), consistent with experiments (Fig. 2*A*).

The 2D simulations provided further insights into spatial dynamics that might be at play during our experiments (Fig. 4*E* and *SI Appendix*, Fig. S10*G*). We observed that sedimentation favored the initial nucleation of dense patches of chemotactic cells, formed at the bottom of the simulation box via chemotaxis toward self-generated gradients of excreted metabolites. These patches later merged and eventually traveled as a band from the bottom to the top of the box, leaving behind a partially depleted medium. Although chemotaxis toward the primary carbon source had itself little importance in our simulations because its gradients were relatively weak (Fig. 4*D* and *SI Appendix*, Fig. S10*G*), chemotaxis toward the secondary nutrient nevertheless increased availability of the primary carbon source to the WT cells since at the later time points both gradients were coincident. Chemotactic response to the primary carbon source became more important when cell sedimentation was assumed to moderately increase in our simulations, which resulted in much steeper carbon source gradients (*SI Appendix*, *Supplementary Text*). Thus, the combination of feeding on higher levels of secondary nutrients and reaching higher levels of the primary carbon source in the upper layer of culture gives the WT cells a growth advantage over the nonchemotactic cells, which were denser at the bottom (*SI Appendix*, Fig. S10*G*).

Discussion

Although microorganisms evolved various regulatory strategies to reallocate their resources dependent on the environment (23), quantitative comparison of costs and benefits of a particular investment strategy for microbial fitness is rarely available. It thus typically remains unclear whether the amount of resources allocated to a particular function follows a specific evolutionary logic of optimization (6). One notable exception here is the regulation of bacterial metabolism, where relative investment into catabolism versus biosynthesis, coordinated by cAMP-CRP signaling, appears to be balanced to maximize growth (1–3, 5). Similarly, at least in some cases, the uptake of a carbon source has been apparently optimized for maximal growth (3). However, bacterial growth on many carbon sources is clearly suboptimal (24), indicating that in those cases the regulation of resource investment did not evolve to maximize growth but rather toward other evolutionary objectives (6). These might include preallocation of resources into biosynthetic or metabolic machinery that may become beneficial when bacteria become suddenly exposed to nutrients, or investment into other functions that are not apparently related to growth (25, 26). Particularly for these latter types of investment, conditions under which they provide fitness benefit and the quantitative relation between the extent and cost of investment and its benefit are unknown.

Here, we investigated costs and benefits of resource allocation into motile behavior, the major cAMP-CRP-dependent cellular function that is not immediately related to *E. coli* growth. Similarly to other cAMP-regulated genes, the expression of motility genes increases linearly with the decrease of growth rate on poorer carbon sources (1, 5). This results in a proportional increase of the length and number of flagellar filaments, and consequently of cell swimming velocity and chemotaxis. The relative fitness cost of motility, i.e., growth disadvantage of motile cells under conditions where motility provides little or no benefit, was also proportionally higher at lower growth rates. This increasing cost was primarily a consequence of higher investment into the biosynthesis of flagella, whereas the cost of swimming was also measurable but lower and only weakly dependent on the growth rate, and the cost the chemotactic signaling was negligible. Thus, linearly increased investment in motility at lower growth rates results in a proportionally linear increase of both the functionality and the cost of motility.

The same negative dependence on the *N*-value of the carbon source was observed for the relative fitness benefit that is provided by chemotaxis, when chemotactic and nonchemotactic cells are cocultured in the presence of nutrient gradients. This dependence could also be seen when expression of chemotaxis and flagellar genes was largely decoupled from the growth rate, implying that increased benefit of chemotaxis at low *N*-values is not the consequence of increased investment but rather due to greater importance of locating additional nutrients when the primary carbon source is poor. The growth-rate dependent regulation of motility genes thus apparently ensures that investment in motility, including chemotaxis, is proportional to the fitness benefit that chemotaxis could provide when nutrient gradients are encountered in a particular carbon source. However, since motility gene regulation was also observed in a shaking culture where gradients cannot form, we conclude that the correlation between potential benefit and investment in motility and chemotaxis is predictive (anticipatory) rather than causal (23). We hypothesize that in the case of chemotaxis such predictive investment might have emerged because chemotaxis operates on a much shorter timescale than gene expression (7) and microscale gradients of nutrients in many natural environments are highly variable and short-lived (27), making direct regulatory coupling of gene expression to the benefit provided by chemotaxis unreliable. Preallocation of increasing amounts of resources in motility and chemotaxis at low growth rates–when the payoffs are likely to be larger—might be a superior strategy, which could explain why motility genes are regulated by cAMP-CRP. The trade-off between the relative fitness benefit and the cost of motility is ultimately dependent on the abundance and quality of encountered nutrient gradients.

The growth-rate dependent fitness benefit of chemotaxis could be observed not only when gradients of nutrients were introduced into bacterial culture, but also in self-generated gradients of the excreted secondary metabolites and of the primary carbon source. Bacterial sedimentation was the likely initial source of nonuniform distribution of bacteria in a culture under our experimental conditions, followed by chemotaxis-dependent redistribution of bacteria toward higher levels of both primary and secondary nutrients. Similar interplay between sedimentation and motility may play an important role in natural (e.g., aquatic) habitats, along with numerous other sources of micro- to mesoscale heterogeneity (28). Excretion of metabolites, including amino acids, sugars, and organic acids into the environment is also a common phenomenon in bacteria and other microorganisms (29). It might serve to optimize proteome allocation during growth (2), but excreted metabolites have also been shown to mediate (mutualistic) metabolic interactions (30) or signaling (31) in various microbial communities, as well as chemotactic self-concentration of bacteria (32–34). Our work thus suggests that chemotaxis may provide a general ecological advantage in competition for reutilization of excreted metabolites, even in communities consisting of single species as long as spatial heterogeneity is allowed to emerge. Such competition for local sources of metabolites is likely to be even more important in structured natural communities (27, 28), and we hypothesize that the regulation of *E. coli* motility has evolved under this selection.

Methods

Detailed description of experimental methods and mathematical modeling can be found in *SI Appendix*.

Data Availability. Metabolomics data and codes used for ODE and PDE simulations are available as Datasets S1–S4.

ACKNOWLEDGMENTS. We thank Thomas Heimerl, Seigo Shima, and Gangfeng Huang for their help with experiments. This research was supported by the Max Planck Society, European Research Council grant 294761-MicRobE to V.S. and Biotechnology and Biological Sciences Research Council grant BB/N00065X/1 to R.G.E.

1. S. Hui *et al*., Quantitative proteomic analysis reveals a simple strategy of global resource allocation in bacteria. *Mol. Syst. Biol.* **11**, 784 (2015).
2. M. Basan *et al*., Overflow metabolism in *Escherichia coli* results from efficient proteome allocation. *Nature* **528**, 99–104 (2015).
3. E. Dekel, U. Alon, Optimality and evolutionary tuning of the expression level of a protein. *Nature* **436**, 588–592 (2005).
4. R. Schuetz, N. Zamboni, M. Zampieri, M. Heinemann, U. Sauer, Multidimensional optimality of microbial metabolism. *Science* **336**, 601–604 (2012).
5. C. You *et al*., Coordination of bacterial proteome with metabolism by cyclic AMP signalling. *Nature* **500**, 301–306 (2013).
6. M. Basan, Resource allocation and metabolism: The search for governing principles. *Curr. Opin. Microbiol.* **45**, 77–83 (2018).
7. H. C. Berg, D. A. Brown, Chemotaxis in *Escherichia coli* analysed by three-dimensional tracking. *Nature* **239**, 500–504 (1972).
8. S. Bi, V. Sourjik, Stimulus sensing and signal processing in bacterial chemotaxis. *Curr. Opin. Microbiol.* **45**, 22–29 (2018).
9. R. Colin, V. Sourjik, Emergent properties of bacterial chemotaxis pathway. *Curr. Opin. Microbiol.* **39**, 24–33 (2017).
10. R. Milo, P. Jorgensen, U. Moran, G. Weber, M. Springer, BioNumbers–The database of key numbers in molecular and cell biology. *Nucleic Acids Res.* **38**, D750–D753 (2010).
11. B. Ni *et al*., Evolutionary remodeling of bacterial motility checkpoint control. *Cell Rep.* **18**, 866–877 (2017).
12. M. Liu *et al*., Global transcriptional programs reveal a carbon source foraging strategy by *Escherichia coli*. *J. Biol. Chem.* **280**, 15921–15927 (2005).
13. J. Adler, B. Templeton, The effect of environmental conditions on the motility of *Escherichia coli*. *J. Gen. Microbiol.* **46**, 175–184 (1967).
14. A. Celani, M. Vergassola, Bacterial strategies for chemotaxis response. *Proc. Natl. Acad. Sci. U.S.A.* **107**, 1391–1396 (2010).
15. N. W. Frankel *et al*., Adaptability of non-genetic diversity in bacterial chemotaxis. *eLife* **3**, e03526 (2014).
16. M. Scott, C. W. Gunderson, E. M. Mateescu, Z. Zhang, T. Hwa, Interdependence of cell growth and gene expression: Origins and consequences. *Science* **330**, 1099–1102 (2010).
17. S. F. Elena, R. E. Lenski, Evolution experiments with microorganisms: The dynamics and genetic bases of adaptation. *Nat. Rev. Genet.* **4**, 457–469 (2003).
18. H. A. de Boer, L. J. Comstock, M. Vasser, The *tac* promoter: A functional hybrid derived from the *trp* and *lac* promoters. *Proc. Natl. Acad. Sci. U.S.A.* **80**, 21–25 (1983).
19. Y. Yang *et al*., Relation between chemotaxis and consumption of amino acids in bacteria. *Mol. Microbiol.* **96**, 1272–1282 (2015).
20. R. Hermsen, H. Okano, C. You, N. Werner, T. Hwa, A growth-rate composition formula for the growth of *E.coli* on co-utilized carbon substrates. *Mol. Syst. Biol.* **11**, 801 (2015).
21. V. Sourjik, A. Vaknin, T. S. Shimizu, H. C. Berg, In *vivo* measurement by FRET of pathway activity in bacterial chemotaxis. *Methods Enzymol.* **423**, 365–391 (2007).
22. D. P. Clark, The fermentation pathways of *Escherichia coli*. *FEMS Microbiol. Rev.* **5**, 223–234 (1989).
23. T. J. Perkins, P. S. Swain, Strategies for cellular decision-making. *Mol. Syst. Biol.* **5**, 326 (2009).
24. B. D. Towbin *et al*., Optimality and sub-optimality in a bacterial growth law. *Nat. Commun.* **8**, 14123 (2017).
25. E. J. O'Brien, J. Utrilla, B. O. Palsson, Quantification and classification of *E. coli* proteome utilization and unused protein costs across environments. *PLoS Comput. Biol.* **12**, e1004998 (2016).
26. M. Mori, S. Schink, D. W. Erickson, U. Gerland, T. Hwa, Quantifying the benefit of a proteome reserve in fluctuating environments. *Nat. Commun.* **8**, 1225 (2017).
27. R. Stocker, J. R. Seymour, Ecology and physics of bacterial chemotaxis in the ocean. *Microbiol. Mol. Biol. Rev.* **76**, 792–812 (2012).
28. O. X. Cordero, M. S. Datta, Microbial interactions and community assembly at microscales. *Curr. Opin. Microbiol.* **31**, 227–234 (2016).
29. N. Paczia *et al*., Extensive exometabolome analysis reveals extended overflow metabolism in various microorganisms. *Microb. Cell Fact.* **11**, 122 (2012).
30. O. Ponomarova *et al*., Yeast creates a niche for symbiotic lactic acid bacteria through nitrogen overflow. *Cell Syst.* **5**, 345–357.e6 (2017).
31. C. S. Pereira, J. A. Thompson, K. B. Xavier, AI-2-mediated signalling in bacteria. *FEMS Microbiol. Rev.* **37**, 156–181 (2013).
32. E. O. Budrene, H. C. Berg, Dynamics of formation of symmetrical patterns by chemotactic bacteria. *Nature* **376**, 49–53 (1995).
33. S. Park *et al*., Motion to form a quorum. *Science* **301**, 188 (2003).
34. L. Laganenka, R. Colin, V. Sourjik, Chemotaxis towards autoinducer 2 mediates autoaggregation in *Escherichia coli*. *Nat. Commun.* **7**, 12984 (2016).